The American Journal of Pathology, Vol. 173, No. 4, October 2008

DOI: 10.2353/ajpath.2008.080237

Matrix Pathobiology

Thrombospondin-1 and CD47 Limit Cell and Tissue Survival of Radiation Injury

Jeff S. Isenberg,* Justin B. Maxhimer,* Fuminori Hyodo,† Michael L. Pendrak,* Lisa A. Ridnour,† William G. DeGraff,† Maria Tsokos,* David A. Wink,† and David D. Roberts*

From the Laboratory of Pathology and the Radiation Biology Branch,† Center for Cancer Research, National Cancer Institute, National Institutes of Health, Bethesda, Maryland*

Radiation, a primary mode of cancer therapy, acutely damages cellular macromolecules and DNA and elicits stress responses that lead to cell death. The known cytoprotective activity of nitric oxide (NO) is blocked by thrombospondin-1, a potent antagonist of NO/cGMP signaling in ischemic soft tissues, suggesting that thrombospondin-1 signaling via its receptor CD47 could correspondingly increase radiosensitivity. We show here that soft tissues in thrombospondin-1-null mice are remarkably resistant to radiation injury. Twelve hours after 25-Gy hindlimb irradiation, thrombospondin-1-null mice showed significantly less cell death in both muscle and bone marrow. Two months after irradiation, skin and muscle units in null mice showed minimal histological evidence of radiation injury and near full retention of mitochondrial function. Additionally, both tissue perfusion and acute vascular responses to NO were preserved in irradiated thrombospondin-1-null hindlimbs. The role of thrombospondin-1 in radiosensitization is specific because thrombospondin-2-null mice were not protected. However, mice lacking CD47 showed radioresistance similar to thrombospondin-1-null mice. Both thrombospondin-1- and CD47-dependent radiosensitization is cell autonomous because vascular cells isolated from the respective null mice showed dramatically increased survival and improved proliferative capacity after irradiation *in vitro*. Therefore, thrombospondin-1/CD47 antagonists may have selective radioprotective activity for normal tissues. ***(Am J Pathol 2008, 173:1100–1112; DOI: 10.2353/ajpath.2008.080237)***

Radiation remains a primary mode of cancer therapy, with one half of newly diagnosed cancer patients receiving some form of radiation therapy. Free radicals generated by ionizing radiation acutely damage cellular DNA and other cellular macromolecules, eliciting stress responses that ultimately lead to cell death.[1] Because DNA damage compromises the ability of cells to undergo mitosis, the tissues most sensitive to effects of radiation are generally those undergoing rapid proliferation. Several mechanisms contribute to radiation-induced cell death including mitotic death, apoptosis, and cell cycle arrest. The mechanism and extent of cell death depend on cell type, cell environment, and the radiation dose. Bystander effects of the direct radiation damage can lead to additional cell death through either direct cell contact or release of intracellular mediators.[2] Ultimately, radiation damage results in death of both cancer and normal cells. Therefore, limiting toxicity to adjacent normal tissues restricts the therapeutic dosage of radiation that can be delivered to a given tumor.

In addition to using three-dimensional conformal radiation therapy to maximize radiation delivery to tumor versus adjacent healthy tissues,[3] a second approach to improve the therapeutic window for radiotherapy involves use of chemical radiosensitizers or radioprotectants. General chemical radiosensitizers or pathway-specific sensitizers such as histone deacetylase inhibitors or inhibitors of Ras signaling have been used to increase the radiosensitivity of tumors.[4–6] Conversely, amifostine and nitroxides such as Tempol have demonstrated radioprotective activities for adjacent tissues.[4,7]

Tissues might also produce endogenous radioprotectants in response to radiation injury. Nitric oxide (NO) is a primary regulator of mammalian physiology. Radiation increases NO production in vascular cells, and NO

Supported by the Intramural Research Program of the National Institutes of Health, National Cancer Institute, Center for Cancer Research (to D.D.R., M.T., D.A.W.).

Accepted for publication July 7, 2008.

Supplemental material for this article can be found on *http://ajp.amjpathol.org*.

Address reprint requests to David D. Roberts, Ph.D., National Institutes of Health, Building 10, Room 2A33, 10 Center Dr., MSC1500, Bethesda, MD 20892-1500. E-mail: droberts@helix.nih.gov.

can protect cells and tissues from radiation damage by stimulating soluble guanylate cyclase production of cGMP to promote cell survival pathways and by several cGMP-independent effector pathways.[8–10] Consistent with these studies, pretreatment of mice with exogenous NO prolongs their survival after a lethal dose of whole body irradiation.[11] However, studies using iNOS inducers and NOS inhibitors indicate that elevated NO production can also contribute to radiation injury.[12] Furthermore, *NOS2* gene transfer into tumors increased their radiosensitivity,[13] and *NOS1*-null mice show increased radioresistance in bone marrow.[14] These apparently conflicting observations could be rationalized if the effects of NO on radiation injury are biphasic and the radioprotective activity of NO occurs at low doses, which typically involve cGMP signaling.

We recently reported that the matricellular protein, thrombospondin-1 (TSP1) blocks NO-stimulated activation of soluble guanylate cyclase.[15,16] and that this process requires engagement of the cell surface receptor CD47.[17] Targeting TSP1 or CD47 enhances ischemic tissue survival and blood flow.[18–20] CD47 engagement may also induce apoptosis of some cell types independent of NO.[21,22] These studies suggested that inhibition of NO signaling by TSP1 might limit the radioprotective activity of NO. We tested this hypothesis using TSP1- and CD47-null mice and demonstrate here that the absence of these proteins significantly improves tissue survival of radiation. Furthermore, we demonstrate that the radiosensitizing activity of TSP1 signaling via CD47 is cell autonomous.

Materials and Methods

Animals

Wild-type, TSP1-null, and CD47-null mice in C57BL/6 background were housed in a pathogen-free environment and had *ad libitum* access to standard rat chow and water. TSP2-null male mice 12 weeks of age and age-matched wild-type B6129sf1/J control animals were obtained from The Jackson Laboratory (Bar Harbor, ME). Care and handling of animals was in compliance with standards established by the Animal Care and Use Committee of the National Cancer Institute.

Reagents and Cells

Primary murine vascular endothelial cells were harvested from wild-type, TSP1-, CD47-, and TSP2-null mice and cultured as previously described in endothelial growth media (Lonza, Basel, Switzerland).[15] Murine B16F10 melanoma cells were kindly provided by Dr. Lyuba Varticovski (National Cancer Institute) and grown in RPMI with 10% fetal calf serum (Life Technologies, Inc., Grand Island, NY).

Irradiation of Mice

Age- and sex-matched wild-type, TSP1-, CD47-, and TSP2-null mice underwent local irradiation to the right hindlimb as previously described.[23] Briefly animals (anesthetized using isofluorine) were placed in customized Lucite jigs that allow for immobilization and selective irradiation of the leg. A single radiation dose of 25 Gy was delivered by a Therapax DXT300 X-ray irradiator (Pantak, Inc., East Haven, CT) using 2.0-mm Al filtration (300 kVp) at a dose rate of 2.53 Gy/minute. Care was taken to avoid irradiation of other body parts by using lead shields specifically designed as a part of the jigs. After irradiation, the animals were placed in cages as indicated above and observed daily for 8 weeks at which time animals were euthanized and tissues fixed in formalin 10% for further analysis. In other experiments, mice receiving 25 Gy to the hindlimb were euthanized 12 hours later and hindlimbs fixed in 10% formalin. Unstained tissue sections were prepared on charged slides from paraffin-embedded hindlimbs for *in situ* analysis of apoptosis as described.

Radiation Growth Delay Assay

C57BL/6 wild-type and TSP1-null 12-week-old female mice were inoculated with syngeneic B16F10 melanoma cells (2.5×10^6 cells/animal) to the right lateral thigh. When tumor volume reached 200 mm^3 half of each group underwent 10 Gy irradiation to the tumor-bearing limb. Tumor size was measured with calipers bi-weekly by the same investigator. Tumor volume was calculated by the formula: volume $= W^2 \times L/2$, where W = shortest diameter and L = longest diameter. Animals were sacrificed if tumors exceeded 2 cm^3 or at 26 days. Results are from 16 animals, 8 of each strain.

Irradiation of Cells

Primary murine lung-derived endothelial cells were plated in standard growth medium in 96- or 6-well culture plates (Nunc, Roskilde, Denmark) and allowed to adhere. Irradiation was done on an X-Rad 320 (Precision X-Ray, East Haven, CT) operating at 300 kV/10 mA with a 2-mm aluminum filter. The dose rate at 50 cm from the X-ray source was 242 cGy/minute, as determined by multiple thermoluminescent dosimeter readings.

Skin Reaction

Skin reaction after hindlimb irradiation was quantified every week after treatment for 8 weeks using a previously described grading system.[24] The grading system consisted of five categories: normal, hair loss, erythema, dry desquamation, and moist desquamation/ulceration.

Leg Contraction Assay

Measurement of hindlimb extension was performed as previously described with modification.[23] Animals were placed under light general anesthesia with 1% isoflurane via nose cone, and the pelvis was immobilized against a post fixed to the examination table. The treated and untreated limbs were then placed individually under a defined degree of tension and the distance of extension measured.

Blood Oxygen Level-Dependent (BOLD) Magnetic Resonance Imaging (MRI) Imaging

MRI images were acquired using a 4.7 T scanner (Bruker Biospin, Billerica, MA) and isoflurane anesthesia. Muscle tissue scanned was at rest, so alterations in oxygenation reflected changes in perfusion rather than in oxygen consumption. MR measurements were started after the mouse's body temperature reached 37°C. Before the experiments, gradient echo-based T_1 sequence was used to determine the target slice location. A series of T_2*-weighted gradient echo BOLD image data sets transverse to the midpoint of the femur were repeatedly acquired for 30 minutes to monitor temporal changes in blood oxygenation and blood flow. Diethylamine-NONOate (DEA/NO, 100 nmol/g body weight) was injected with saline via the rectal cannula 5.0 minutes after starting the scan. Imaging parameters used were: TR = 450 ms, Flip angle = 45, Nex = 1, slice thickness = 2 mm, matrix size = 64 × 64, total imaging time for the series was 29 minutes.

Laser Doppler Analysis

Hindlimb flow was measured using laser Doppler imaging (MoorLD1-2λ; Moor Instruments, Devon, UK). Briefly, animals were placed in a supine position on a heating pad, and anesthesia was provided by 1% inhalation isoflurane in a 50:50 mixture of oxygen to room air. Core temperature was monitored by rectal probe and was further controlled with a heat lamp. The hair of the ventral surface of the anterior abdominal wall or respective hindlimb was clipped and depiliated with Nair, Church and Dwight Co, Princeton, NJ, and a region of interest marked. After equilibration to the experimental set-up baseline hindlimb blood flow was measured. The following instrument settings were used: override distance 21 cm; scan time 4 milliseconds/pixel. Results are expressed as the change percent control from baseline of the region of interest.

Mitochondrial DNA Analysis

Primer sequences were derived using FastPCR (*http://www.primerdigital.com/index.php?page = 35*, last accessed June 12, 2007) and were chosen to amplify ~100-bp regions of unique genomic and mitochondrial genes using quantitative polymerase chain reaction (PCR). DNA was quantified by measuring fluorescent intensity using Taq polymerase amplification in a SYBR green reaction mixture (Thermo Fisher Scientific, Waltham, MA) with an MJ Research Opticon I instrument (Bio-Rad, Hercules, CA). Data were processed using the Opticon I software supplied with the instrument. Melting curve analysis was performed for each sample to ensure a single product was produced in each reaction. The cycling parameters consisted of an initial denaturation at 95°C for 15 minutes, followed by 40 cycles of denaturation at 94°C and annealing at 60°C for 20 seconds each with extension for 30 seconds at 72°C, ending with a final extension at 72°C for 10 minutes. Melting temperatures were determined in 0.2°C steps from 60 to 95°C with a dwell time of 8 seconds. Gene copy number was assessed using twofold dilutions of genomic DNA samples from mouse muscle tissue samples. Samples were normalized using *PKD1* as an internal control standard. The gene identification numbers are listed followed by the coordinates of the first gene primer. *PKD1* polycystin 1 NT_039649.6(nuclear), 0917160 5′-ACCGACTCAACCAGGCCACAG-3′, 5′-GGAGGTCCATTGTGCCCATGG-3′; *GTF2IRD1* general transcription factor, NT_039314 (nuclear), 4559250 5′-AGGGACCGCCTCCACAAGCTG-3′, 5′-TCTCCGTGCAGGAACTGGCTG-3′; *Osteocalcin* NM_001032298.2 (nuclear), 255 5′-ACCCTGCTTGTGACG-3′, 5′-GCTTTAGGGCAGCACAGGTCC-3′; *NADH6* NC_005089.1 (mitochondrial), 13587 5′-CCGCAAACAAAGATCACCCAG-3′, 5′-GTTGGAGTTATGTTGGAAGGAGG-3′; and *16S rRNA* NC_005089.1 (mitochondrial) 1432, 5′-GCTTGGTGATAGCTGGTTACC-3′, 5′-TCCGTTCCAGAAGAGCTGTCC-3′.

Cell Survival Assay

Wild-type, TSP-1-null, and CD47-null or TSP2-null and wild-type B6129sf1/J lung-derived endothelial cells were resuspended in Endothelial growth medium and seeded into 96-well plates (Nunc) at a density of 5×10^3 cells/200 μl per well and incubated for 24 hours at 37°C. Cells were then exposed to a single dose of gamma radiation (0, 10, 20, 30, and 40 Gray) and allowed to incubate another 72 hours at 37°C. Cell viability was determined with the CellTiter 96 Aqueous One Solution cell proliferation assay (Promega, Madison, WI) as per the manufacturer's instructions and absorbance at 490 nm determined using an MR580 Microelisa AutoReader (Dynatech, Alexandria, VA).

Cell Proliferation Assay

Proliferation was assessed by quantifying incorporation of bromodeoxyuridine (BrdU) into newly synthesized DNA using a BrdU cell proliferation assay (Calbiochem, La Jolla, CA). Primary murine wild-type, TSP1-, TSP2-, and CD47-null lung endothelial cells were seeded into 96 well plates at 5×10^4 cells/well density. After 24 hours of incubation at 37°C treatment groups were irradiated at 40 Gy. Control and irradiated plates were assayed for BrdU uptake throughout 24 hours starting at 48 to 168 hours after radiation. The assay was performed according to the manufacturer's protocol, and the plates were read at 420 nm.

Mitochondrial Viability Assay

Mitochondrial viability of hindlimb muscle biopsies was assessed by the reduction of a tetrazolium salt to water-insoluble formazan through mitochondrial oxidation as described.[19] Results were expressed as absorbance normalized to dry tissue weight.

Tissue Apoptosis

The ApopTag *in situ* detection kit (Chemicon, Millipore, MA) was used following the manufacturer's recommendations. In brief, sections undergo deparaffinization, rehydration, and washing, followed by treatment with 20 μg/ml of proteinase K for 15 minutes at room temperature and repeat washing. Endogenous peroxidase activity was quenched with 3% H_2O_2 in phosphate-buffered saline (PBS) for 5 minutes. The 3′-hydroxy DNA strand breaks were enzymatically labeled with digoxygenin nucleotide via TdT and incubated for 1 hour at 37°C, and the reaction terminated with a stop buffer. Sections were then incubated with anti-digoxygenin peroxidase for 30 minutes at room temperature, washed, stained with 3–3′-diaminobenzidine substrate, counterstained with methyl green and mounted. Positive and negative control slides provided with the kit are used in each assay to ensure consistency.

Histology

Tissue units were excised, fixed in 10% buffered formaldehyde, paraffin-embedded, and sectioned at a thickness of 5 μm. Sections were then stained with hematoxylin and eosin (H&E). Review of each slide was performed by an independent pathologist blinded to the origin of each tissue slide.

Immunohistochemistry

Paraffin-embedded hindlimbs were sectioned at a thickness of 5 μm and applied to charged glass slides and processed for immunohistology. Tissue sections were deparaffinized with xylene and rehydrated in alcohol. Slides were then heat-inactivated in 10 mmol/L sodium citrate (pH 6.0) in a microwave for 5 minutes. Cooled slides were rinsed with PBS and then incubated with 3% H_2O_2 for 30 minutes at room temperature. Sections were then blocked with 5% normal goat serum in PBS for 30 minutes at room temperature followed by a 12-hour incubation in a humidified chamber at 37°C with a monoclonal CD31 antibody (clone JC70A; DakoCytomation, Glostrup, Denmark) at a 1:40 dilution. Slides were washed and then incubated with secondary antibody, washed, and incubated in prediluted streptavidin-horseradish peroxidase conjugate (BD PharMingen, Franklin Lakes, NJ). Color was developed by a diaminobenzidine substrate kit (BD PharMingen).

Statistics

All experiments were replicated at least three times. Results are presented as the mean ± SD with analysis of significance done by the Student's *t*-test or one-way analysis of variance with Tukey post hoc test where indicated using Origin software (version 7; OriginLabs Corp., Northhampton, MA), with significance taken at P values <0.05.

Results

TSP1- and CD47-Null Mice Show Tissue Preservation after Radiation Injury

Previous studies identified a role for TSP1 in inducing developmental hair loss during the catagen phase.[25] Extending this observation to radiation alopecia, we observed less hair loss 8 weeks after treatment on the irradiated hindlimbs of TSP1-null mice compared to age- and sex-matched wild-type mice (Figure 1A). An even more dramatic preservation of hair viability was observed for the hindlimbs of irradiated CD47-null mice. Moreover, irradiated skin on the treated null mice showed minimal to no skin ulceration or wet desquamation (Figure 1A). When scored using the grading system of Flanders and colleagues,[23,24] wild-type animals demonstrated both accelerated skin changes and more substantial final changes in skin phenotype compared to null animals (Figure 1B). Histologically, hair follicles and skin architecture were better preserved 8 weeks after irradiation in TSP1-nulls and essentially normal in the CD47-null animals (Figure 1C).

Remarkably, tissue preservation in the irradiated null mice also extended to the underlying skeletal muscle. H&E-stained sections of irradiated wild-type muscle showed significant loss of muscle fibers and nuclei, but these were primarily intact in irradiated tissue sections from TSP1- and CD47-null animals (Figure 1C). Mitochondrial viability in irradiated muscle tissue was assessed by tetrazolium salt reduction (Figure 1D). In contrast to the expected loss of mitochondrial viability in irradiated wild-type muscle, mitochondrial viability assessed 8 weeks after irradiation was significantly greater in muscle biopsies from irradiated hindlimbs in both TSP1- and CD47-null mice, with no significant difference between the irradiated and control limbs in these mice (Figure 1D).

This preservation of mitochondrial function in the TSP1-null mice occurred despite the expected substantial loss in copy number for two mitochondrial genes (*NADH6* and *16S mtRNA*) compared to that for two nuclear genes in the irradiated tissue as expected because of the relatively inefficient DNA repair processes in mitochondria.[26] Selective loss of the mitochondrial genes was similar in the TSP1-nulls (Figure 1E), indicating that TSP1 has no effect on the level of immediate DNA damage caused by radiation or on the subsequent level of mitochondrial DNA repair.

TSP-2 Is Not a Radiosensitizer

In contrast to the TSP1-null mice, TSP2-null mice in a B6129sf1/J background demonstrated significant hair loss and skin damage after radiation at the gross tissue level. Recovery from irradiation did not differ between the TSP2-null and wild-type mice in the same background throughout the 8-week period studied (Figure 2A). Mitochondrial viability in irradiated muscle tissue was assessed by tetrazolium salt reduction and demonstrated a comparable decrease in viability between wild-type and

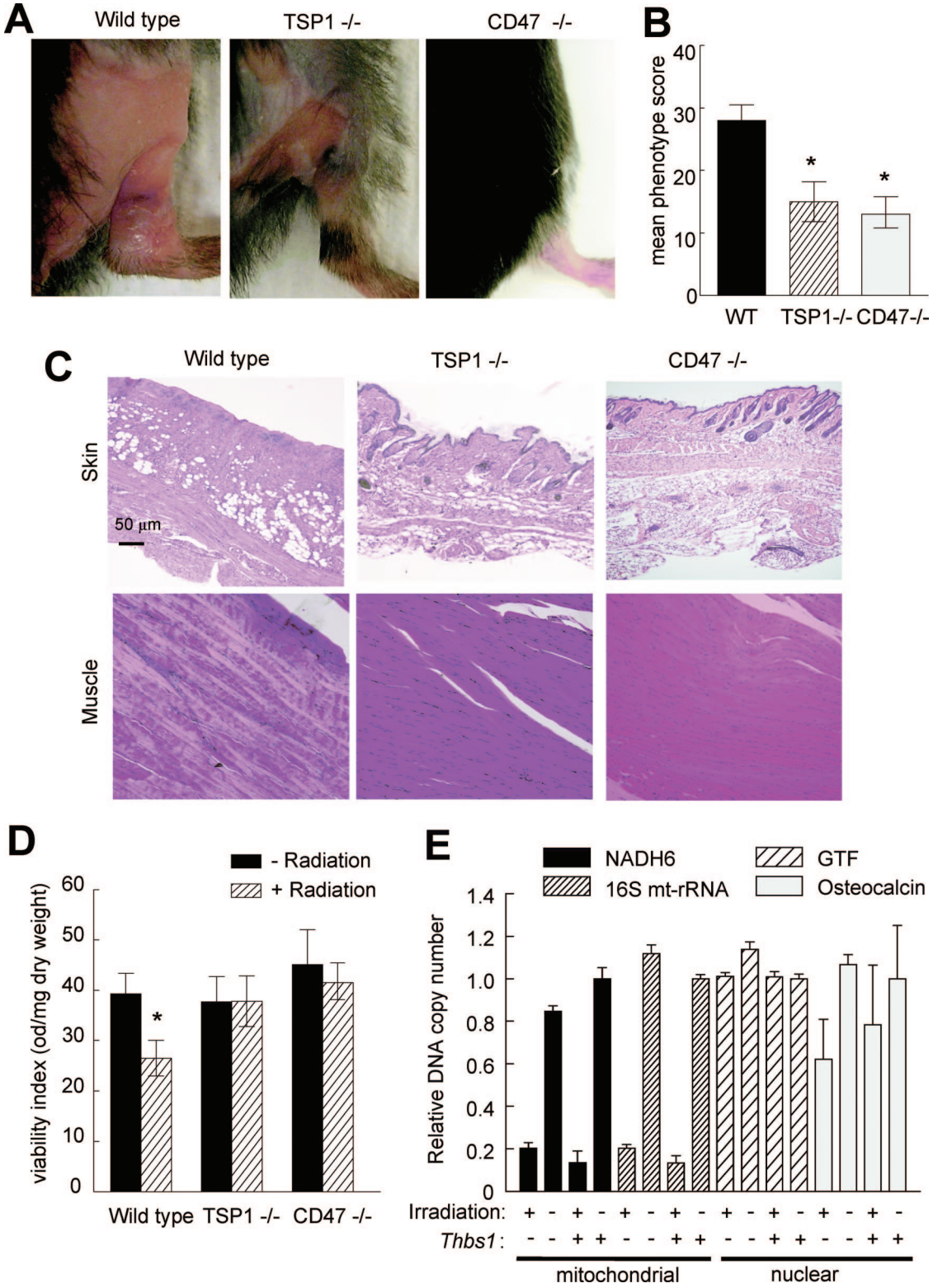

Figure 1. TSP1 and CD47 limit survival of irradiated soft tissue. **A:** Age- and sex-matched C57BL/6 wild-type, TSP1-null, and CD47-null mice received 25 Gy of irradiation to the right hindlimb. **B:** Tissue changes were assessed every week, and scores are presented for 2 months. Significance was determined using the independent two-tailed *t*-test. $^*P < 0.05$ versus wild type. **C:** Representative H&E-stained sections of muscle and skin are shown from irradiated hindlimbs harvested after 2 months. Original magnifications, ×20. **D:** Mitochondrial viability of hindlimb muscle biopsies was assessed at 2 months after irradiation by the reduction of a tetrazolium salt to water insoluble formazan through mitochondrial oxidation as described. Significance was determined using the independent two-tailed *t*-test. $^*P < 0.05$ versus wild-type nonradiated. Results were expressed as absorbance normalized to dry tissue weight. **E:** Copy numbers in control and irradiated muscle tissue harvested at 2 months were determined for two mitochondrial genes (*NADH6* and 16s rRNA, *mt-Rnr2*) and two nuclear genes (the general transcription factor *Gtf2ird1* and osteocalcin, *Bglap2*) by quantitative real-time PCR. For each sample, results were normalized to the nuclear gene *Pkd1*.

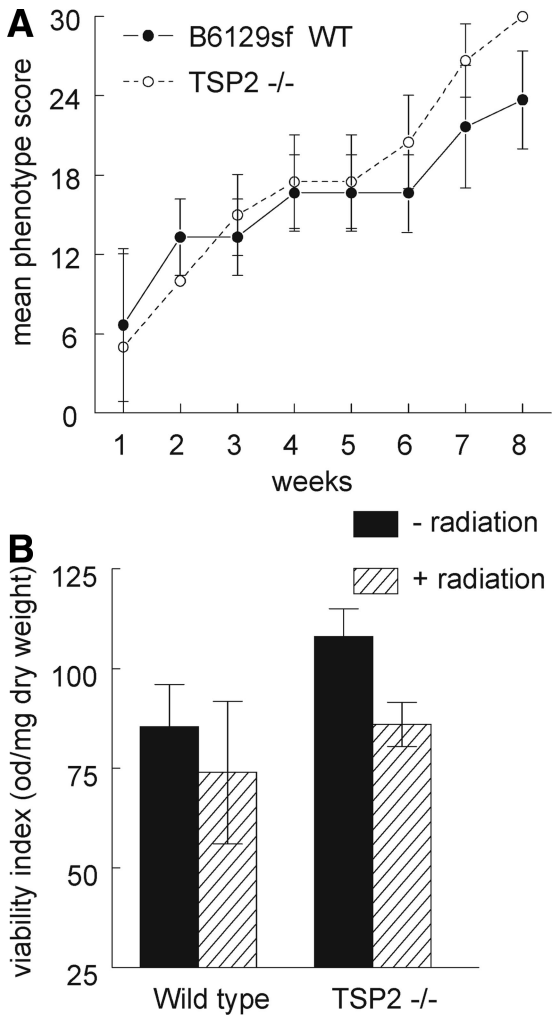

Figure 2. TSP2 does not modulate radiation-induced tissue damage. Age- and sex-matched B6129sf1/J wild-type and TSP2-null mice received 25 Gy to the right hindlimb. **A:** Tissue changes were assessed every week and scored throughout the next 2 months. **B:** Mitochondrial viability of hindlimb muscle biopsies was assessed at 2 months by the reduction of a tetrazolium salt to water insoluble formazan through mitochondrial oxidation as described. Results were expressed as absorbance normalized to dry tissue weight.

TSP2-null muscle samples (Figure 2). H&E-stained sections from irradiated wild-type and TSP2-null hindlimbs showed comparable levels of muscle fiber and nuclei loss, and no tendency toward vascular remodeling was found in TSP2-null irradiated hindlimbs (data not shown).

TSP1- and CD47-Null Mice Demonstrate Enhanced Leg Extension after Radiation Injury

In addition to demonstrating significant resistance to cutaneous injury after radiation, irradiated hindlimbs of TSP1- and CD47-null animals did not show any atrophy at 8 weeks. Rather, there was a tendency toward hypertrophy of the limb soft tissues and vascular elements as compared to irradiated limbs in wild-type animals and control nonirradiated limbs (see Supplemental Figure 1 at *http://ajp.amjpathol.org*). TSP2-null hindlimbs did not show hypertrophy. Limb flexibility, quantified as the maximum degree of limb lengthening, was preserved in

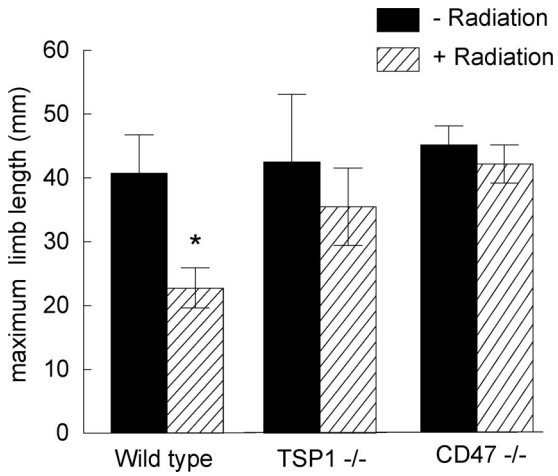

Figure 3. Limb flexibility is preserved in irradiated tissue in the absence of TSP1. Limb extension in age- and sex-matched C57BL/6 wild-type, TSP1-null, and CD47-null mice was measured as described 8 weeks after 25 Gy to the right hindlimb. Significance was determined using the independent two-sample *t*-test. $^*P < 0.05$ versus wild type nonradiated.

TSP1- and CD47-null hindlimbs 8 weeks after 25 Gy of radiation (Figure 3). In contrast, wild-type limbs demonstrated the expected loss of extension.

TSP1 and CD47 Limit Radiation-Induced Alterations in Vascular Response

Two months after 25 Gy of irradiation of the right hindlimb, blood flow responses in both hindlimbs were assessed using BOLD MRI after challenge with a rapidly releasing NO donor (1 μl/g animal weight of 100 mmol/L DEA/NO, Figure 4A). The irradiated hindlimbs in wild-type animals demonstrated an exaggerated overall increase in blood flow compared to the untreated hindlimb. In contrast, the blood flow responses integrated throughout the irradiated and untreated hindlimbs were essentially identical for the first 15 minutes in TSP1-null animals, demonstrating protection from the effects of radiation injury on vascular responsiveness. Multislice multiecho and T2-weighted images confirmed significant tissue changes and injury in wild-type irradiated hindlimbs (Figure 4B). These changes were markedly less in irradiated TSP1-null limbs.

Analysis of areas in the hindlimbs exhibiting positive and negative BOLD signals further emphasized the preservation of normal vascular responses in irradiated TSP1-null hindlimbs (Figure 5). Areas with both positive and negative BOLD signals in irradiated limbs showed more exaggerated responses to NO than corresponding areas in control limbs of wild-type mice. The corresponding areas in irradiated TSP1-null hindlimbs resembled those of the untreated limb, confirming the preservation of normal vascular responsiveness despite radiation injury.

We further examined global vascular perfusion in irradiated hindlimbs using laser Doppler imaging (see Supplemental Figure 2 at *http://ajp.amjpathol.org*). Two months after irradiation, perfusion responses were assessed for 45 minutes after administration of DEA/NO (1 μl/g body weight of a 100 mmol/L stock solution, Figure 6A). Blood flow

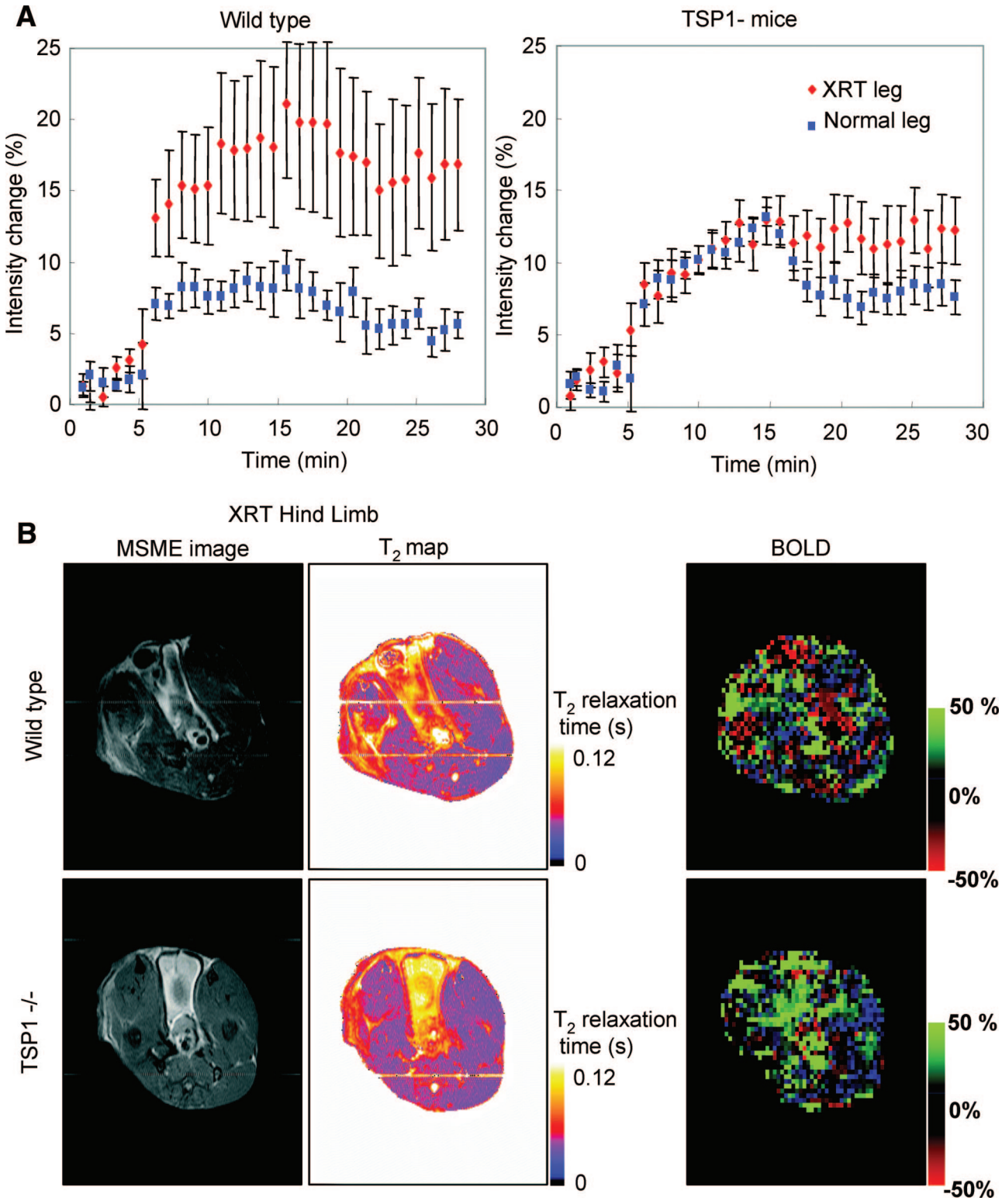

Figure 4. TSP1 limits tissue vascular response after irradiation. **A:** Age- and sex-matched wild-type and TSP1-null mice received 25 Gy to the right hindlimb. Eight weeks later limb perfusion was assessed via BOLD MRI. Images were obtained for 30 minutes from T_2*-weighted gradient echo sequences. DEA/NO (100 nmol/g body weight) was administered 5 minutes after starting the scan. The percent change in integrated BOLD values as a function of time is presented as mean ± SE of eight pairs of wild-type and TSP1-null mice, respectively. **B:** Representative multislice multiecho, T_2 maps, and BOLD images show normal and irradiated hindlimbs of wild-type and TSP1-null animals. In all images, the irradiated (XRT) limb is on the **left**.

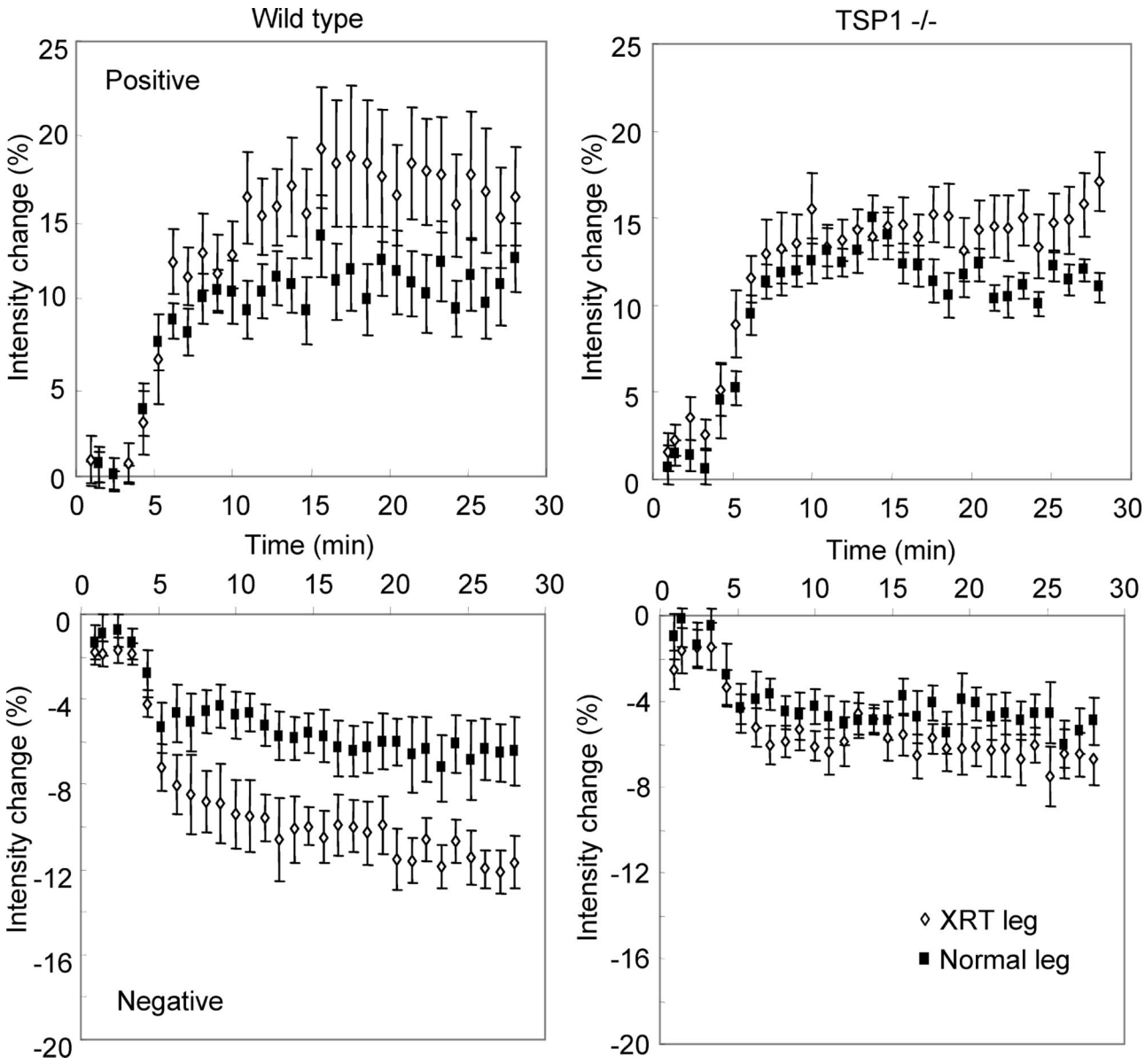

Figure 5. The absence of TSP1 preserves blood oxygenation responses to NO in irradiated hindlimbs. Positive (**top**) and negative (**bottom**) BOLD MRI signal curves are shown after NO treatment for irradiated (**open symbols**) and normal hindlimbs (**filled symbols**) in age- and sex-matched wild-type and TSP1-null 8 weeks after 25 Gy to the right hindlimb.

increased modestly in the irradiated limb of wild-type mice, but significantly greater increases in response to vasoactive challenge were found in TSP1- and CD47-null mice.

Tissue blood flow is dependent directly on vascular density, and increased vascularity could afford a protective advantage after tissue injury. Localized differences in organ vascularity have been reported between wild-type and TSP1- or TSP2-null mice. Enhanced dermal vascularity was noted in TSP1-null pups compared to wild type.[27] However, similar aged pups showed no difference in retinal vascularity until stressed by hyperoxia-induced ischemia.[28] In dermal wound healing, wild-type and TSP1-null tissue sections demonstrated comparable vascularity,[29] in contrast to TSP2-null tissue sections that showed enhanced vessel density. Furthermore, analysis of several visceral organs in wild-type and TSP1-null mice failed to demonstrate significant vascular differences.[30] Quantification of vascular elements in cutaneous units from age- and sex-matched C57BL/6 wild-type, TSP1- and CD47-null, and B6129sfJ and TSP2-null mice failed to document any significant difference in vessel count (Figure 6B). Similarly, immunohistochemical analysis of $CD31^+$ vessels in paraffin-embedded hindlimb sections demonstrated no significant differences between wild-type, TSP1-null, and CD47-null mice (data not shown).

Irradiated Hindlimbs in Null Mice Experience Minimal Apoptosis

To assess the effects of TSP1 and CD47 on radiation-induced apoptosis *in vivo*, *in situ* staining of limb sections to

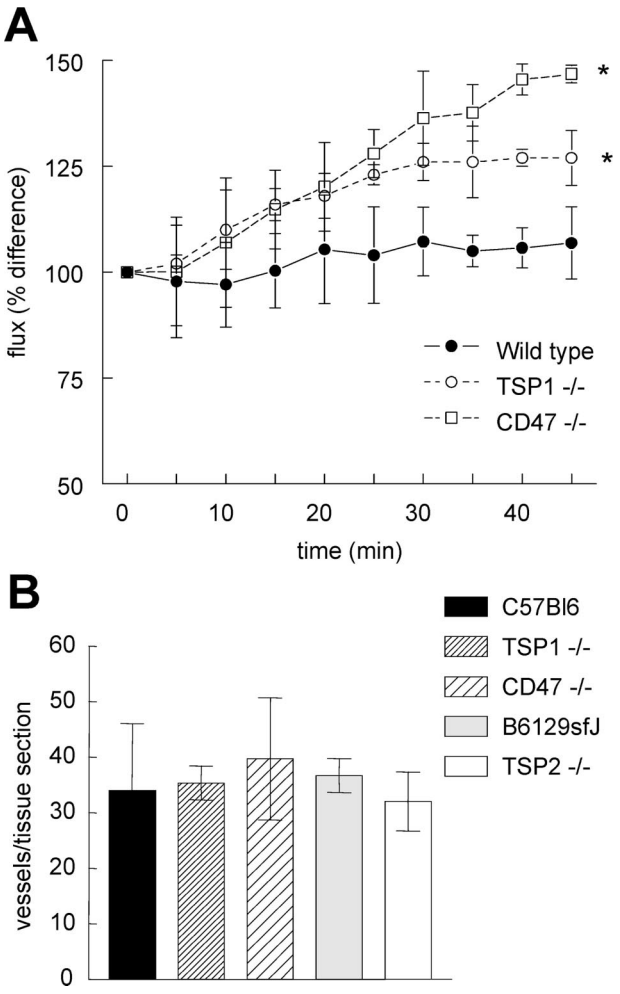

Figure 6. TSP1 and CD47 modulate irradiated hindlimb responses to vasoactive challenge. Age- and sex-matched C57BL/6 wild-type, TSP1-null, and CD47-null mice received 25 Gy irradiation to the right hindlimb. Eight weeks after irradiation, limb perfusion was assessed by laser Doppler imaging for 45 minutes after NO vasoactive challenge (1 μl/g weight 100 mmol/L DEA/NO stock via rectal bolus). **A:** Animals were maintained at a core temperature of 35.5°C and 1.5% isoflurane anesthesia. Significance was determined using the independent two-tailed *t*-test. $^*P < 0.05$ versus wild type. **B:** Cutaneous skin sections 1 × 2 cm in dimension were harvested from age- and sex-matched mice, stained for H&E, and vessels counted.

detect DNA fragmentation was performed on age- and sex-matched wild-type and null mice that received 25 Gy to the hindlimb. Consistent with previous studies,[31] time course experiments in wild-type animals demonstrated maximal tissue staining at 12 hours (data not shown). In contrast, immunohistology of TSP1- and CD47-null limbs after radiation demonstrated minimal to no evidence of apoptosis either in the skeletal musculature or the bone marrow (Figure 7A).

Endogenous TSP1 and CD47 Regulate Radiation-Induced Death of Vascular Cells in Vitro

Improved hindlimb survival in TSP1- and CD47-null mice could result from an intrinsic resistance of cells in the null tissue to irradiation or from a diminished inflammatory response in the nulls that permits better repair of the radiation injury. To differentiate these two hypotheses we assessed the intrinsic radiation sensitivity of primary vascular cells cultured from each strain. Several studies have reported that vascular endothelial cells are highly radiosensitive and so may limit hindlimb survival of irradiation.[32] Primary endothelial cells from lungs of wild-type, TSP1-null, and CD47-null mice were irradiated, and mitochondrial viability was determined by MTT assay 72 hours after injury. Wild-type cells demonstrated radiation dose-dependent cell death that resembled that of human cells (Figure 8A and results not shown). In contrast, doses up to 40 Gy failed to induce significant cell death in TSP1- and CD47-null cells.

Chronic pulmonary inflammation has been reported in TSP1-null mice,[30] and the resulting inflammatory mediators could potentially alter the radiation sensitivity of endothelial cells harvested from this organ. However, the 12-week-old sex-matched mice used in the present study demonstrated no evidence of lung inflammation in any strain based on histological analysis of H&E sections (Figure 7B). Radioprotection in primary cells was specific for loss of TSP1 in that primary TSP2-null endothelial cells were not protected after irradiation (Figure 8B).

TSP1 Limits Endothelial Cell Proliferation after Irradiation

Although the above results show that ablation of TSP1 or CD47 permits cell survival after 40 Gy of irradiation, it was not clear that these cells maintain the ability to proliferate. To assess this, we examined cellular incorporation of BrdU into DNA. Consistent with their limited proliferative capacity in tissue culture, untreated wild-type murine lung endothelial cells showed diminished BrdU uptake with time, and 40 Gy of irradiation further diminished their DNA synthesis. As previously published, TSP1-null cells have an enhanced proliferative capacity,[15] but irradiation of these cells did not significantly decrease DNA synthesis throughout the 7-day time period studied (Figure 8C). Therefore, in addition to promoting survival, the absence of TSP1 permits continued growth of irradiated vascular cells.

Absence of Endogenous TSP1 Does Not Limit Tumor Response to Radiation

Expression of TSP1 by tumor cells is known to limit tumor angiogenesis and growth[33] but not acute blood flow.[34] Conversely, host TSP1 expression can limit B16 tumor growth by inhibiting angiogenesis.[35] Because pretreatment with exogenous TSP1 enhanced the response of a human melanoma xenograft to radiation,[36] we examined whether endogenous host TSP1 could similarly serve as a radiosensitizer. Syngeneic B16F10 melanoma cells were implanted into the hindlimbs of age- and sex-matched wild-type and TSP1-null mice. B16 melanoma cells express very low levels of TSP1 mRNA, and TSP1 protein was reported to be below detectable levels.[37] When the tumors obtained a volume of 200 mm^3, half of the mice of

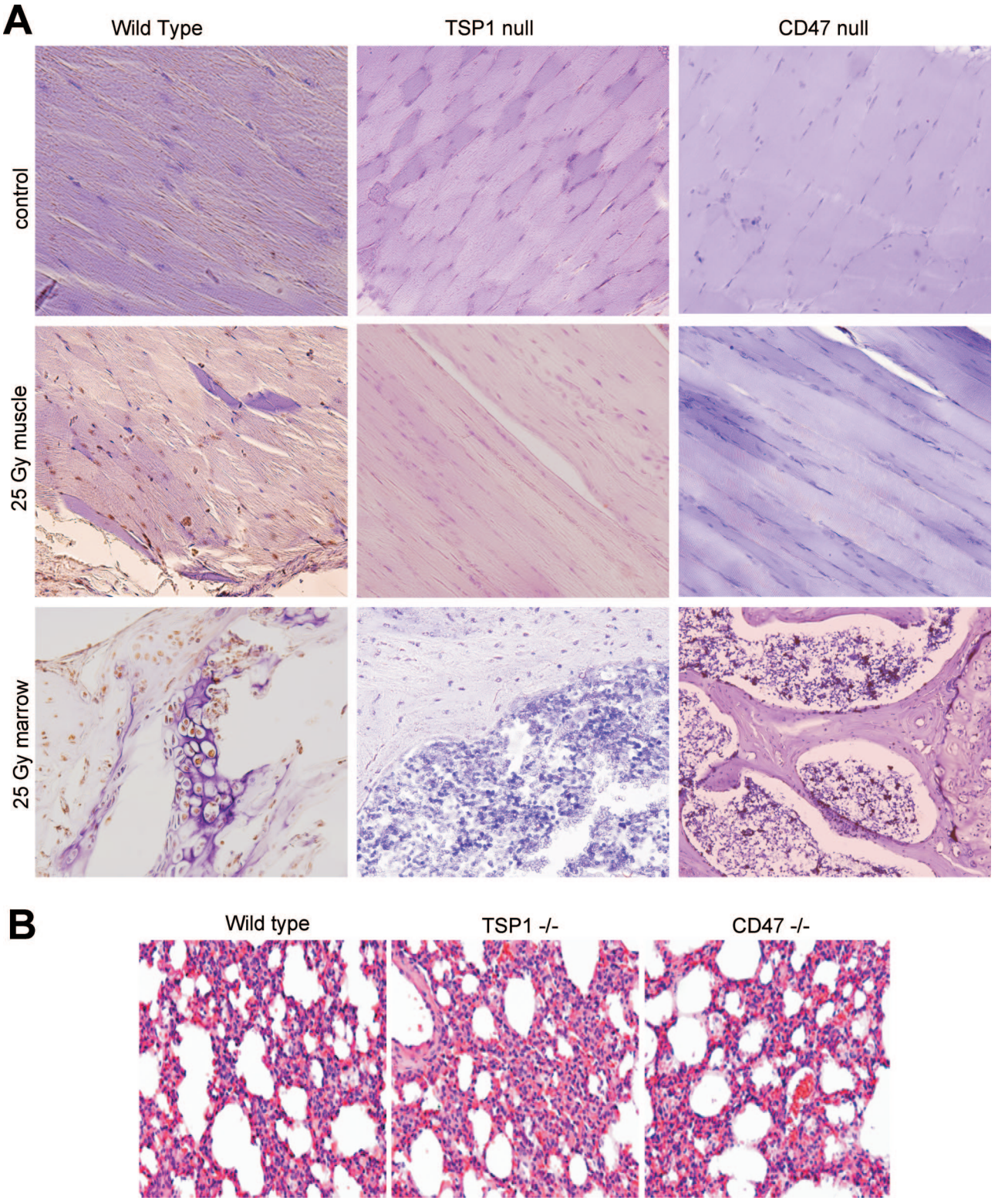

Figure 7. Endogenous TSP1 and CD47 sensitize muscle and bone marrow to radiation-induced apoptosis. **A:** The presence of apoptosis within mouse hindlimb tissue was examined by immunohistochemistry using a peroxidase *in situ* apoptosis detection kit. Nonirradiated control hindlimbs (**top**) and hindlimbs irradiated for a total of 25 Gy from the indicated strains were prepared for paraffin-embedded tissue sections 12 hours after radiation and were examined for the presence of apoptotic nuclei. Apoptosis is inferred by intranuclear staining of muscle and bone marrow cells. Images were acquired using a ×20 objective. **B:** Lungs were obtained from 12-week-old wild-type, TSP1-null, and CD47-null mice and stained for H&E. Original magnifications, ×100.

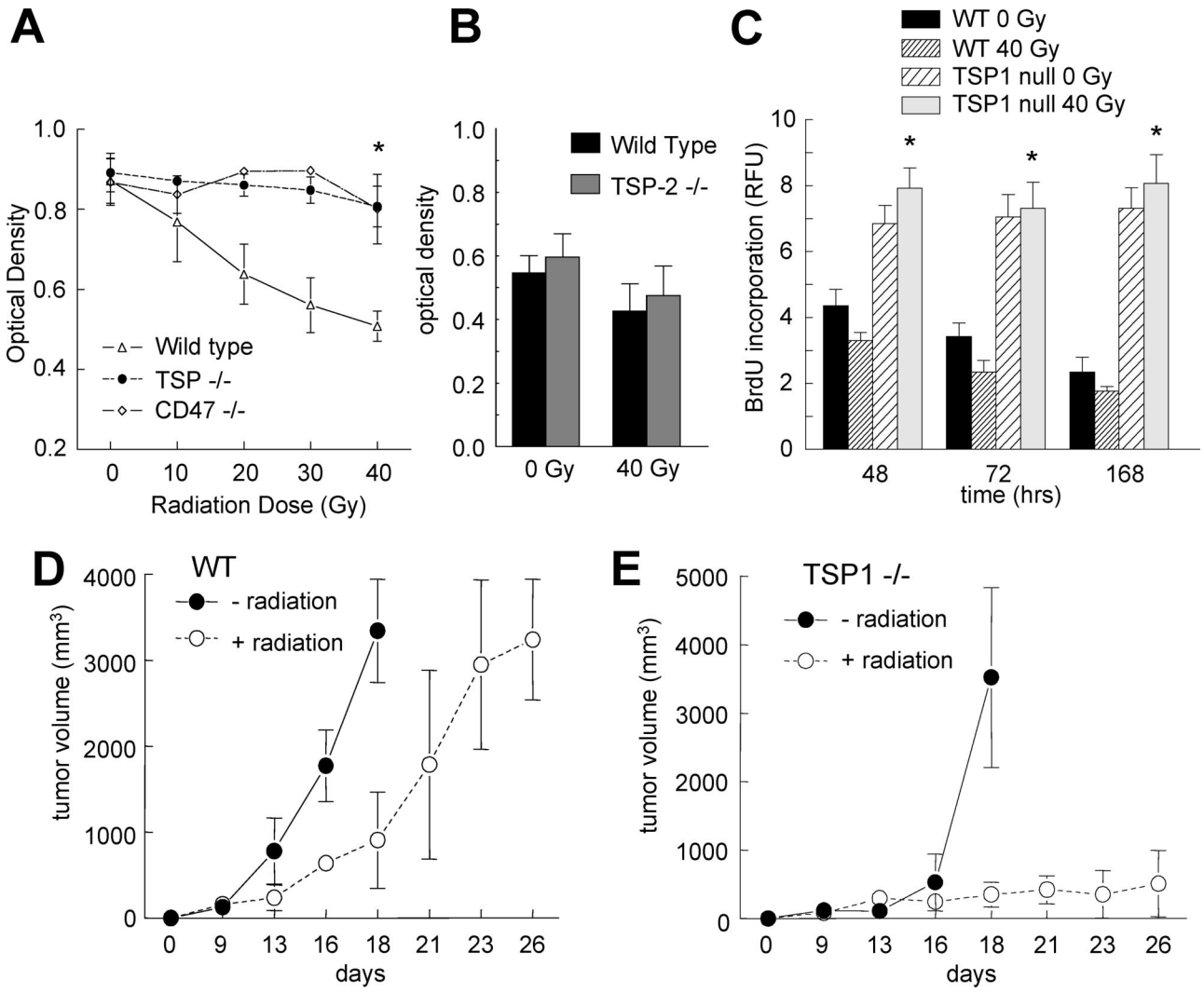

Figure 8. TSP1 and CD47 limit vascular cell survival and proliferation after radiation. **A:** Primary vascular endothelial cells were harvested as previously described from wild-type, TSP1-null, and CD47-null mice and plated in growth medium on 96-well culture plates (5×10^3 cells/200 μl per well), treated with the indicated doses of radiation, and cell viability determined by MTT assay at 72 hours. Significance was determined using the independent two-tailed *t*-test. $^*P < 0.05$ versus wild type. **B:** Primary vascular endothelial cells were harvested from wild-type and TSP2-null mice and plated in growth medium on 96-well culture plates (5×10^3 cells/200 μl per well), treated with the indicated doses of radiation and cell viability determined by MTT assay after 72 hours of incubation. Primary murine wild-type and TSP1 vascular endothelial cells were seeded into 96-well plates at 5×10^4 cells/well density. After 24 hours cells were then either irradiated at 40 Gy or left to incubate at 37°C as a control. **C:** At the indicated time points after irradiation, proliferation was assessed by quantifying incorporation of BrdU into new synthesized DNA using a BrdU cell proliferation assay (Calbiochem, La Jolla, CA). Results are presented as relative fluorescence units (RFUs), and significance was determined using the one-way analysis of variance test. $^*P < 0.05$ versus wild type. C57BL/6 wild-type (**D**) and TSP1-null 12-week-old female mice (**E**) were inoculated with B16F10 melanoma cells (2.5×10^6 cells/animal) to the right lateral thigh. On tumors reaching 200 mm^3 half of each group underwent 10 Gy of radiation to the tumor-bearing limb. Tumor size was measured bi-weekly. Animals were sacrificed if tumors exceeded 2 cm^3. Results are from 16 animals, 8 of each strain.

each strain received 10 Gy of irradiation to the tumor-bearing hindlimb. Tumors in both wild-type and TSP1-null animals demonstrated a significant growth delay after radiation (Figure 8, D and E). The delay was somewhat longer in the null, suggesting that therapies to protect normal tissue by blocking TSP1/CD47 signaling would not impair radiotherapy of the tumor.

Discussion

Off target damage to noncancerous tissues and vital organs remains one of the primary limitations for applying radiation therapy to treat cancer. One effort to enhance the therapeutic potential for radiotherapy while minimizing its complications has centered on developing radioprotectants. We herein identify TSP1 and CD47 as limiting components of a cell-autonomous signaling pathway that controls tissue survival after high-dose irradiation. The therapeutic potentials of this pathway are substantial. Targeting this pathway may enhance the therapeutic window for radiotherapy of cancer by radioprotection of healthy tissue. Agents that block this radiosensitization pathway could also be valuable to limit the toxic effects of accidental radiation exposure.

Radiation-induced tissue damage and vascular dysregulation was evident in irradiated wild-type and TSP2-

null hindlimbs but minimal in irradiated TSP1-null and CD47-null hindlimbs. Enhanced cell survival and proliferation correlated with tissue preservation at the gross and microscopic levels in both TSP1- and CD47-null animals, an advantage also not realized in irradiated TSP2-null mice. Tissue preservation translated into improved functional status 8 weeks after irradiation. Functional benefits to the irradiated tissue beds included decreased hair loss, cutaneous desquamation and ulceration, tissue contracture, and ischemia. These long-term benefits appear to result from an acute survival advantage of the null genotypes because both tissue and bone marrow apoptosis were drastically reduced in the null mice within 1 day after the radiation injury. In the absence of TSP1/CD47 signaling, vascular cells cultured from the respective null mice showed enhanced cell survival and proliferative capacity after radiation injury, demonstrating that this acute radioprotection of vascular cells is cell-autonomous.

Damage to DNA is an immediate and universal effect of radiation. As expected, endogenous TSP1 does not prevent this immediate damage as assessed by similar loss of mitochondrial DNA in wild-type and null irradiated tissue. DNA damage in turn initiates both cell repair pathways and cell death via p53-dependent and p53-independent mechanisms. Because TSP1 signaling via CD47 is known to induce caspase-independent type III cell death in leukocytes,[22] the absence of TSP1 or CD47 may prevent radiation-induced cell death through a similar mechanism. This combined with enhancement of prosurvival NO/cGMP signaling could account for the cell-autonomous radioprotection of the null vascular cells. The protection from radiation-induced damage *in vivo*, however, probably involves additional functions of TSP1 and CD47. CD47 is required for leukocyte recruitment,[38] and TSP1 is also known to stimulate T-cell migration.[39] Therefore, TSP1- and CD47-null mice also might benefit from decreased leukocyte recruitment during the acute response to radiation injury.

Endothelial cells are exquisitely sensitive to radiation-induced cell death through the induction of several mediators of apoptosis.[32] Within 24 hours of irradiation, damaged capillaries demonstrate leukocyte attachment, endothelial cell swelling, thrombosis with complete loss of capillary networks, and secondary ischemia. Even vessels that remain patent undergo long-term thickening of the basement membrane and soft tissue scarring. This late effect is driven by activation of fibroblasts by radiation through the terminal differentiation of progenitor cells into postmitotic fibrocytes and elevated production of collagen by the same.[32,40] These processes depend on transforming growth factor (TGF)-β, and TSP1 is a mediator of latent TGF-β activation[41] and TGF-β-dependent fibrosis.[42] Deletion of *Smad3* in mice is protective for radiation-induced fibrosis by blocking TGF-β signaling.[23] Thus, TSP1-null mice may be partially protected from the long-term fibrotic response to radiation, but this does not explain the immediate protection of the TSP1-null, and we would not expect CD47-null mice to share this TGF-β-dependent benefit.

Although TSP1- and CD47-null endothelial cells and mice show a dramatic resistance to radiation, TSP2-null cells and mice showed no significant protection against radiation-induced cell death or tissue damage. This was surprising because TSP1 and TSP2 share a number of cellular receptors, and both are potent angiogenesis inhibitors. TSP2 was inferred to interact with CD47 based on conservation of a CD47-binding peptide sequence identified in TSP1 and a shared immune phenotype of TSP1- and TSP2-null mice.[43,44] However, uncertainties concerning structural basis for TSP1-CD47 interaction raise questions about whether TSP2 also interacts with this receptor.[45] Lack of radioprotection in the TSP2-null could arise either from lack of TSP2 binding to CD47 or lack of significant TSP2 expression at an appropriate time after radiation injury.

Deletion of several other genes in transgenic mice has been associated with increased (*Nos1*, *Smad3*, *Chk2*, *p53*) or decreased radioresistance (*cKit*, *p53*) of bone marrow or intestinal crypt cells to whole body irradiation or to irradiation of cells *in vitro*.[14,46–48] However, less attention has been given to identifying genes that modulate the radiosensitivity of skin and other soft tissues that can be dose-limiting for radiotherapy of tumors and complicate reconstructive surgery after irradiation.

Thbs1 or *CD47* deletion dramatically improves hindlimb resistance to high-dose irradiation and vascular cell survival of irradiation *in vitro*. This suggests that strategies to prevent TSP1/CD47 interaction or to suppress expression of either protein could enhance the radioresistance of soft tissues. Our preliminary studies in TSP1-null mice demonstrate that tumors in these mice retain their sensitivity to radiation. Therefore, TSP1/CD47 antagonists may have selective radioprotective activity for normal tissues. However, additional studies are needed to determine whether therapeutic blockade of TSP1-CD47 in wild-type mice would influence the sensitivity of tumors to ionizing radiation under these conditions and to address whether the beneficial effects of this pathway extend to the late tissue damage associated with irradiation.

Acknowledgments

We thank Dr. Larry Keefer for providing reagents and Dr. Murali Krishna for guidance in design and analysis of the MRI imaging studies.

References

1. Chapman JD: Single-hit mechanism of tumour cell killing by radiation. Int J Radiat Biol 2003, 79:71–81
2. Prise KM, Schettino G, Folkard M, Held KD: New insights on cell death from radiation exposure. Lancet Oncol 2005, 6:520–528
3. Purdy JA: From new frontiers to new standards of practice: advances in radiotherapy planning and delivery. Front Radiat Ther Oncol 2007, 40:18–39
4. Poggi MM, Coleman CN, Mitchell JB: Sensitizers and protectors of radiation and chemotherapy. Curr Probl Cancer 2001, 25:334–411
5. Karagiannis TC, El-Osta A: Modulation of cellular radiation responses by histone deacetylase inhibitors. Oncogene 2006, 25:3885–3893
6. McKenna WG, Muschel RJ, Gupta AK, Hahn SM, Bernhard EJ: The RAS signal transduction pathway and its role in radiation sensitivity. Oncogene 2003, 22:5866–5875
7. Cotrim AP, Hyodo F, Matsumoto K, Sowers AL, Cook JA, Baum BJ, Krishna MC, Mitchell JB: Differential radiation protection of salivary glands versus tumor by Tempol with accompanying tissue assess-

ment of Tempol by magnetic resonance imaging. Clin Cancer Res 2007, 13:4928–4933
8. Freeman SL, MacNaughton WK: Nitric oxide inhibitable isoforms of adenylate cyclase mediate epithelial secretory dysfunction following exposure to ionising radiation. Gut 2004, 53:214–221
9. Leach JK, Black SM, Schmidt-Ullrich RK, Mikkelsen RB: Activation of constitutive nitric-oxide synthase activity is an early signaling event induced by ionizing radiation. J Biol Chem 2002, 277:15400–15406
10. Zhong GZ, Chen FR, Bu DF, Wang SH, Pang YZ, Tang CS: Cobalt-60 gamma radiation increased the nitric oxide generation in cultured rat vascular smooth muscle cells. Life Sci 2004, 74:3055–3063
11. Liebmann J, DeLuca AM, Coffin D, Keefer LK, Venzon D, Wink DA, Mitchell JB: In vivo radiation protection by nitric oxide modulation. Cancer Res 1994, 54:3365–3368
12. Ohta S, Matsuda S, Gunji M, Kamogawa A: The role of nitric oxide in radiation damage. Biol Pharm Bull 2007, 30:1102–1107
13. Cook T, Wang Z, Alber S, Liu K, Watkins SC, Vodovotz Y, Billiar TR, Blumberg D: Nitric oxide and ionizing radiation synergistically promote apoptosis and growth inhibition of cancer by activating p53. Cancer Res 2004, 64:8015–8021
14. Epperly MW, Cao S, Zhang X, Franicola D, Shen H, Greenberger EE, Epperly LD, Greenberger JS: Increased longevity of hematopoiesis in continuous bone marrow cultures derived from NOS1 (nNOS, mt-NOS) homozygous recombinant negative mice correlates with radioresistance of hematopoietic and marrow stromal cells. Exp Hematol 2007, 35:137–145
15. Isenberg JS, Ridnour LA, Perruccio EM, Espey MG, Wink DA, Roberts DD: Thrombospondin-1 inhibits endothelial cell responses to nitric oxide in a cGMP-dependent manner. Proc Natl Acad Sci USA 2005, 102:13141–13146
16. Isenberg JS, Wink DA, Roberts DD: Thrombospondin-1 antagonizes nitric oxide-stimulated vascular smooth muscle cell responses. Cardiovasc Res 2006, 71:785–793
17. Isenberg JS, Ridnour LA, Dimitry J, Frazier WA, Wink DA, Roberts DD: CD47 is necessary for inhibition of nitric oxide-stimulated vascular cell responses by thrombospondin-1. J Biol Chem 2006, 281:26069–26080
18. Isenberg JS, Hyodo F, Pappan LK, Abu-Asab M, Tsokos M, Krishna MC, Frazier WA, Roberts DD: Blocking thrombospondin-1/CD47 signaling alleviates deleterious effects of aging on tissue responses to ischemia. Arterioscler Thromb Vasc Biol 2007, 27:2582–2588
19. Isenberg JS, Hyodo F, Matsumoto K, Romeo MJ, Abu-Asab M, Tsokos M, Kuppusamy P, Wink DA, Krishna MC, Roberts DD: Thrombospondin-1 limits ischemic tissue survival by inhibiting nitric oxide-mediated vascular smooth muscle relaxation. Blood 2007, 109:1945–1952
20. Isenberg JS, Romeo MJ, Abu-Asab M, Tsokos M, Oldenborg A, Pappan L, Wink DA, Frazier WA, Roberts DD: Increasing survival of ischemic tissue by targeting CD47. Circ Res 2007, 100:712–720
21. Manna PP, Dimitry J, Oldenborg PA, Frazier WA: CD47 augments Fas/CD95-mediated apoptosis. J Biol Chem 2005, 280:29637–29644
22. Bras M, Yuste VJ, Roue G, Barbier S, Sancho P, Virely C, Rubio M, Baudet S, Esquerda JE, Merle-Beral H, Sarfati M, Susin SA: Drp1 mediates caspase-independent type III cell death in normal and leukemic cells. Mol Cell Biol 2007, 27:7073–7088
23. Flanders KC, Sullivan CD, Fujii M, Sowers A, Anzano MA, Arabshahi A, Major C, Deng C, Russo A, Mitchell JB, Roberts AB: Mice lacking Smad3 are protected against cutaneous injury induced by ionizing radiation. Am J Pathol 2002, 160:1057–1068
24. Flanders KC, Major CD, Arabshahi A, Aburime EE, Okada MH, Fujii M, Blalock TD, Schultz GS, Sowers A, Anzano MA, Mitchell JB, Russo A, Roberts AB: Interference with transforming growth factor-beta/Smad3 signaling results in accelerated healing of wounds in previously irradiated skin. Am J Pathol 2003, 163:2247–2257
25. Yano K, Brown LF, Lawler J, Miyakawa T, Detmar M: Thrombospondin-1 plays a critical role in the induction of hair follicle involution and vascular regression during the catagen phase. J Invest Dermatol 2003, 120:14–19
26. Prithivirajsingh S, Story MD, Bergh SA, Geara FB, Ang KK, Ismail SM, Stevens CW, Buchholz TA, Brock WA: Accumulation of the common mitochondrial DNA deletion induced by ionizing radiation. FEBS Lett 2004, 571:227–232
27. Crawford SE, Stellmach V, Murphy-Ullrich JE, Ribeiro SM, Lawler J, Hynes RO, Boivin GP, Bouck N: Thrombospondin-1 is a major activator of TGF-beta1 in vivo. Cell 1998, 93:1159–1170
28. Wang S, Wu Z, Sorenson CM, Lawler J, Sheibani N: Thrombospondin-1-deficient mice exhibit increased vascular density during retinal vascular development and are less sensitive to hyperoxia-mediated vessel obliteration. Dev Dyn 2003, 228:630–642
29. Bornstein P, Agah A, Kyriakides TR: The role of thrombospondins 1 and 2 in the regulation of cell-matrix interactions, collagen fibril formation, and the response to injury. Int J Biochem Cell Biol 2004, 36:1115–1125
30. Lawler J, Sunday M, Thibert V, Duquette M, George EL, Rayburn H, Hynes RO: Thrombospondin-1 is required for normal murine pulmonary homeostasis and its absence causes pneumonia. J Clin Invest 1998, 101:982–992
31. Mazur L, Augustynek A, Halicka HD, Deptala A: Induction of apoptosis in bone marrow cells after treatment of mice with WR-2721 and gamma-rays: relationship to the cell cycle. Cell Biol Toxicol 2003, 19:13–27
32. Rodemann HP, Blaese MA: Responses of normal cells to ionizing radiation. Semin Radiat Oncol 2007, 17:81–88
33. Weinstat-Saslow DL, Zabrenetzky VS, VanHoutte K, Frazier WA, Roberts DD, Steeg PS: Transfection of thrombospondin 1 complementary DNA into a human breast carcinoma cell line reduces primary tumor growth, metastatic potential, and angiogenesis. Cancer Res 1994, 54:6504–6511
34. Isenberg JS, Hyodo F, Ridnour LA, Shannon CS, Wink DA, Krishna MC, Roberts DD: Thrombospondin-1 and vasoactive agents indirectly alter tumor blood flow. Neoplasia 2008, 10:886–896
35. Lawler J, Miao WM, Duquette M, Bouck N, Bronson RT, Hynes RO: Thrombospondin-1 gene expression affects survival and tumor spectrum of p53-deficient mice. Am J Pathol 2001, 159:1949–1956
36. Rofstad EK, Henriksen K, Galappathi K, Mathiesen B: Antiangiogenic treatment with thrombospondin-1 enhances primary tumor radiation response and prevents growth of dormant pulmonary micrometastases after curative radiation therapy in human melanoma xenografts. Cancer Res 2003, 63:4055–4061
37. Culp WD, Tsagozis P, Burgio M, Russell P, Pisa P, Garland D: Interference of macrophage migration inhibitory factor expression in a mouse melanoma inhibits tumor establishment by up-regulating thrombospondin-1. Mol Cancer Res 2007, 5:1225–1231
38. Lindberg FP, Bullard DC, Caver TE, Gresham HD, Beaudet AL, Brown EJ: Decreased resistance to bacterial infection and granulocyte defects in IAP-deficient mice. Science 1996, 274:795–798
39. Li Z, Calzada MJ, Sipes JM, Cashel JA, Krutzsch HC, Annis DS, Mosher DF, Roberts DD: Interactions of thrombospondins with alpha4beta1 integrin and CD47 differentially modulate T cell behavior. J Cell Biol 2002, 157:509–519
40. Brush J, Lipnick SL, Phillips T, Sitko J, McDonald JT, McBride WH: Molecular mechanisms of late normal tissue injury. Semin Radiat Oncol 2007, 17:121–130
41. Murphy-Ullrich JE, Poczatek M: Activation of latent TGF-beta by thrombospondin-1: mechanisms and physiology. Cytokine Growth Factor Rev 2000, 11:59–69
42. Belmadani S, Bernal J, Wei CC, Pallero MA, Dell'italia L, Murphy-Ullrich JE, Berecek KH: A thrombospondin-1 antagonist of transforming growth factor-beta activation blocks cardiomyopathy in rats with diabetes and elevated angiotensin II. Am J Pathol 2007, 171:777–789
43. Gao AG, Lindberg FP, Finn MB, Blystone SD, Brown EJ, Frazier WA: Integrin-associated protein is a receptor for the C-terminal domain of thrombospondin. J Biol Chem 1996, 271:21–24
44. Lamy L, Foussat A, Brown EJ, Bornstein P, Ticchioni M, Bernard A: Interactions between CD47 and thrombospondin reduce inflammation. J Immunol 2007, 178:5930–5939
45. Carlson CB, Lawler J, Mosher DF: Thrombospondins: from structure to therapeutics: structures of thrombospondins. Cell Mol Life Sci 2008, 65:672–686
46. Komarova EA, Kondratov RV, Wang K, Christov K, Golovkina TV, Goldblum JR, Gudkov AV: Dual effect of p53 on radiation sensitivity in vivo: p53 promotes hematopoietic injury, but protects from gastrointestinal syndrome in mice. Oncogene 2004, 23:3265–3271
47. Epperly MW, Goff JP, Zhang X, Niu Y, Shields DS, Wang H, Shen H, Franicola D, Bahnson AB, Nie S, Greenberger EE, Greenberger JS: Increased radioresistance, g(2)/m checkpoint inhibition, and impaired migration of bone marrow stromal cell lines derived from Smad3(−/−) mice. Radiat Res 2006, 165:671–677
48. Takai H, Naka K, Okada Y, Watanabe M, Harada N, Saito S, Anderson CW, Appella E, Nakanishi M, Suzuki H, Nagashima K, Sawa H, Ikeda K, Motoyama N: Chk2-deficient mice exhibit radioresistance and defective p53-mediated transcription. EMBO J 2002, 21:5195–5205